Supporting Information for: Vibrations and Phase Stability in Mixed Valence Antimony Oxide

Duncan H. Moseley,[†] Rinkle Juneja,[†] Luke L. Daemen,[‡] Ilya Sergueev,[¶] René Steinbrügge,[¶] Olaf Leupold,[¶] Yongqiang Cheng,[§] Valentino R. Cooper,[†] Lucas Lindsay,[†] Michelle K. Kidder,[∥] Michael E. Manley,[†] and Raphaël P. Hermann[*,†]

[†]*Materials Science and Technology Division, Oak Ridge National Laboratory, Oak Ridge, TN 37831, USA*

[‡]*Neutron Scattering Division, Oak Ridge National Laboratory, Oak Ridge, TN 37831, USA*

[¶]*Deutsches Elektronen-Synchrotron DESY, D-22607 Hamburg, Germany*

[§]*Neutron Science Division, Oak Ridge National Laboratory, Oak Ridge, TN 37831, USA*

[∥]*Manufacturing Science Division, Oak Ridge National Laboratory, Oak Ridge, TN 37831, USA*

E-mail: hermannrp@ornl.gov

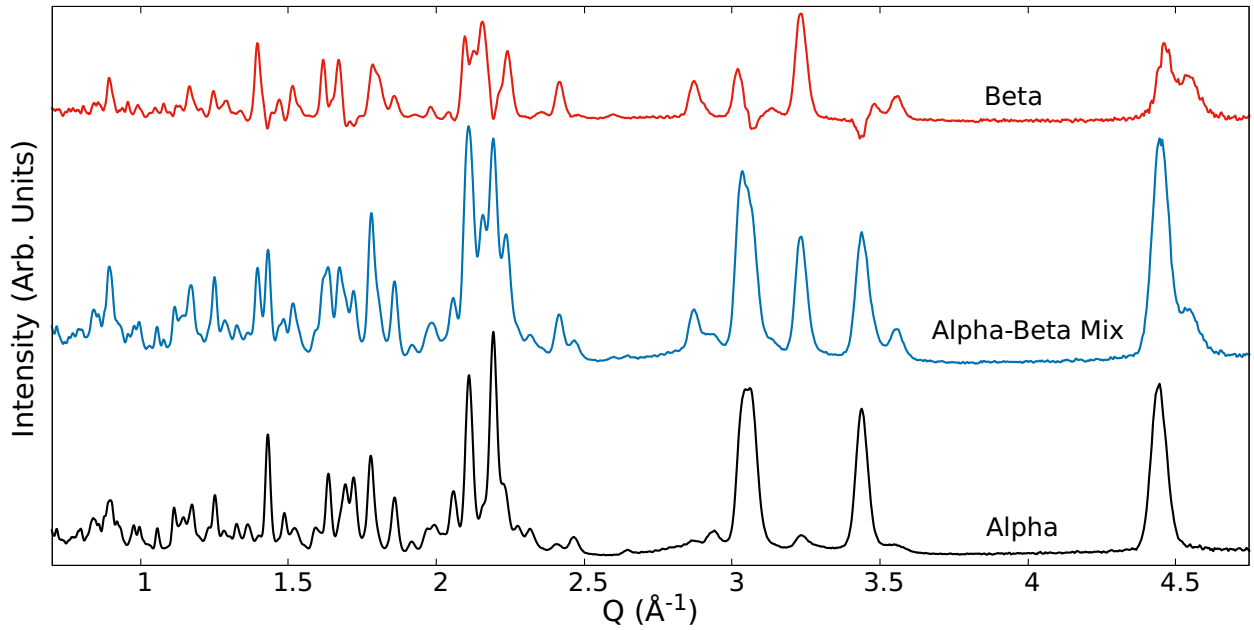

Figure S1: Powder neutron diffraction data collected at the VISION spectrometer of α-Sb_2O_4, mixed-phase Sb_2O_4, and β-Sb_2O_4 determined by subtracting the pure α phase from the mixed phase.

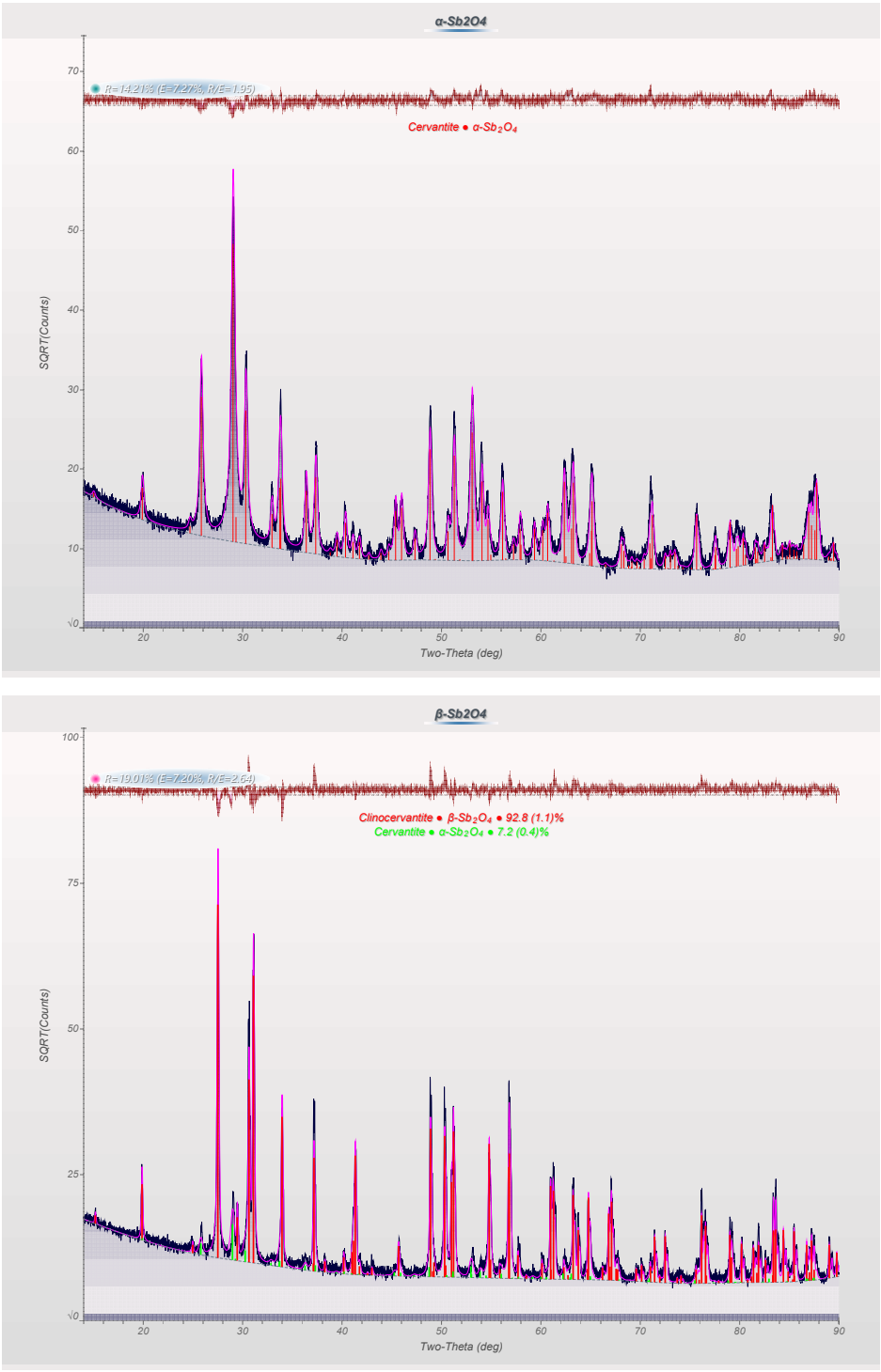

Figure S2: Powder x-ray diffraction data of both phases of (top) α-Sb_2O_4 and (bottom) β-Sb_2O_4.

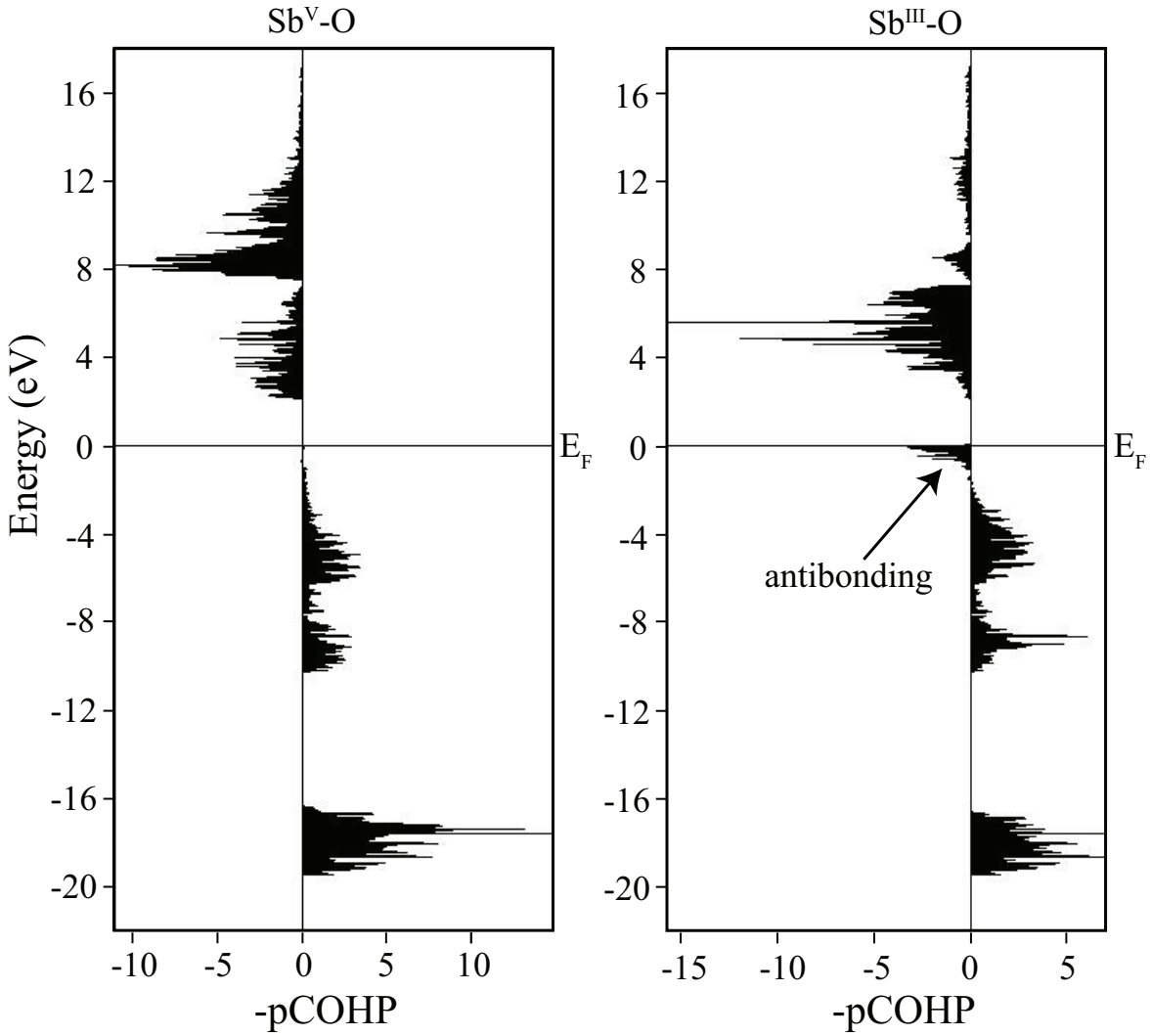

Figure S3: Energy vs COHP for (left) Sb^{V}-O and (right) Sb^{III}-O pairs in α-Sb_2O_4. Note that Sb^{V} type corresponds to Sb1-Sb4, as labeled in Figure S5 (a).

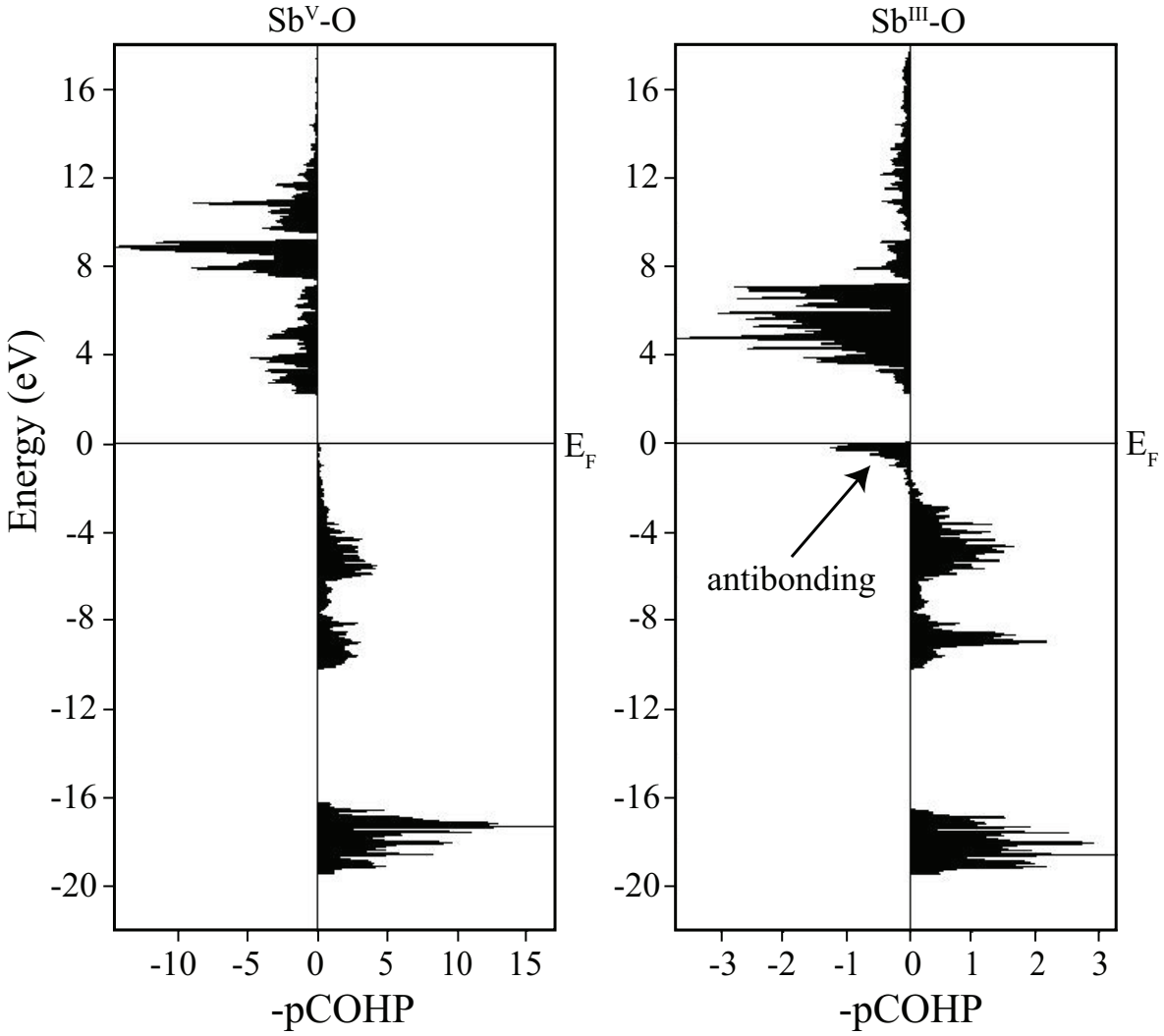

Figure S4: Energy vs COHP for (left) Sb^{V}-O and (right) Sb^{III}-O pairs in β-Sb_2O_4. Note that Sb^{V} type correspond to Sb1-Sb4, as labeled in Figure S5 (b).

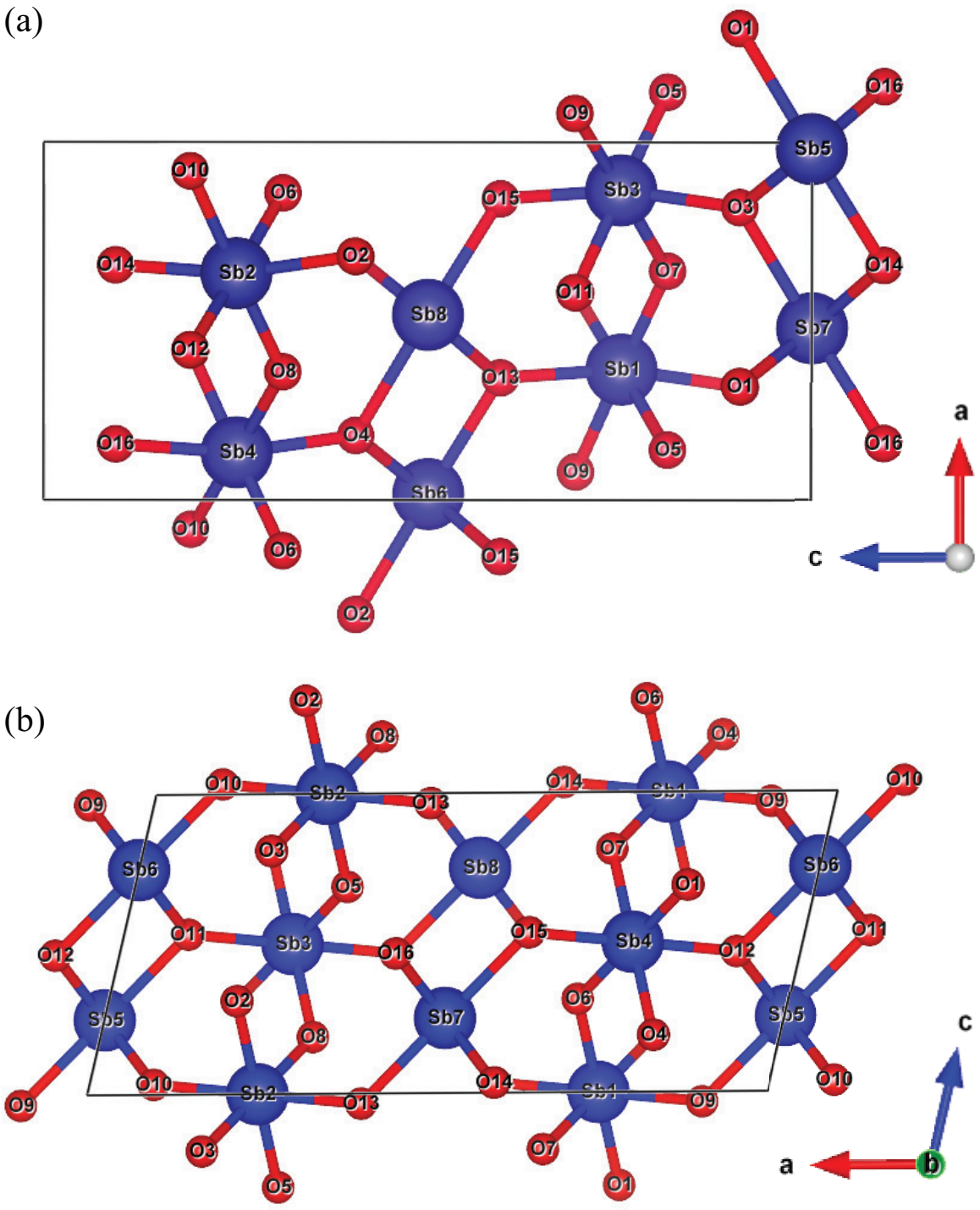

Figure S5: Conventional unit cell of (a) α-Sb_2O_4 and (b) β-Sb_2O_4 with site labels for Sb and O atoms.

Table S1: ICOHP contribution to the band structure energy for Sb^{V}-O pairs for α-Sb_2O_4. The site labels are shown in Figure S5 (a).

Sb^{V}-O pair	ICOHP
Sb1-O1	-0.00472
Sb1-O5	-5.35259
Sb1-O7	-5.75696
Sb1-O9	-0.00601
Sb1-O11	-0.01992
Sb1-O13	-4.81139
Sb2-O2	-0.00472
Sb2-O6	-5.35259
Sb2-O8	-5.75696
Sb2-O10	-0.00601
Sb2-O12	-0.01992
Sb2-O14	-4.81139
Sb3-O3	-5.06866
Sb3-O5	-0.00465
Sb3-O7	-5.35259
Sb3-O9	-0.00420
Sb3-O11	-5.23881
Sb3-O15	-4.81139
Sb4-O4	-5.06866
Sb4-O6	-0.00465
Sb4-O8	-5.35259
Sb4-O10	-0.00420
Sb4-O12	-5.23881
Sb4-O16	-4.81139

Table S2: ICOHP contribution to the band structure energy for Sb^{V}-O pairs for β-Sb_2O_4. The site labels are shown in Figure S5 (b).

Sb^{V}-O pair	ICOHP
Sb1-O1	-0.00851
Sb1-O4	-0.01703
Sb1-O6	-5.46395
Sb1-O7	-0.00330
Sb1-O9	-0.00124
Sb1-O14	-4.94247
Sb2-O2	-5.46382
Sb2-O3	-0.01231
Sb2-O5	-0.00845
Sb2-O8	-5.52113
Sb2-O10	-4.94245
Sb2-O13	-0.00125
Sb3-O2	-0.01704
Sb3-O3	-5.46395
Sb3-O5	-5.52113
Sb3-O8	-5.46380
Sb3-O11	-4.94247
Sb3-O16	-4.94246
Sb4-O1	-0.01703
Sb4-O4	-5.46404
Sb4-O6	-5.52111
Sb4-O7	-5.46389
Sb4-O12	-4.94246
Sb4-O15	-4.94245

Table S3: Experimental (Amador et al. - Ref. [20]) and calculated lattice constants and angles for α-Sb_2O_4 and β-Sb_2O_4. The α phase is orthorhombic and all angles are 90°.

Compound	Method	a (Å)	b (Å)	c (Å)
α-Sb_2O_4	Exp	5.434(1)	4.8091(6)	11.779(2)
α-Sb_2O_4	DFT	5.57	4.90	11.93
β-Sb_2O_4	Exp	12.057(1)	4.8352(3)	5.384(2)
β-Sb_2O_4	DFT	12.19	4.92	5.52
		α (degrees)	β (degrees)	γ (degrees)
β-Sb_2O_4	Exp	90.00	104.56(1)	90.00
β-Sb_2O_4	DFT	90.00	103.39	90.00

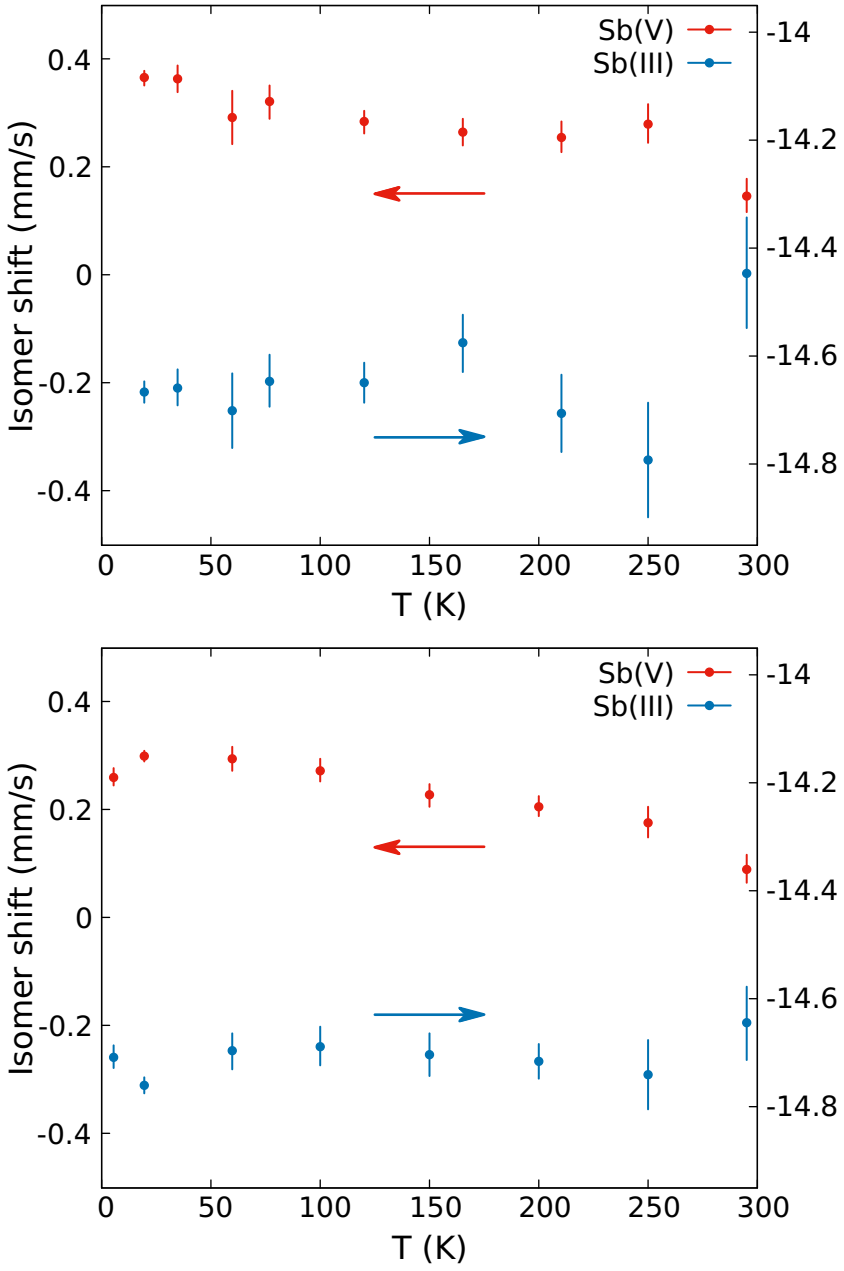

Figure S6: (a) Temperature-dependence of isomer shifts of the Sb^{III} and Sb^{V} ions in (top) α- and (bottom) β-Sb_2O_4.

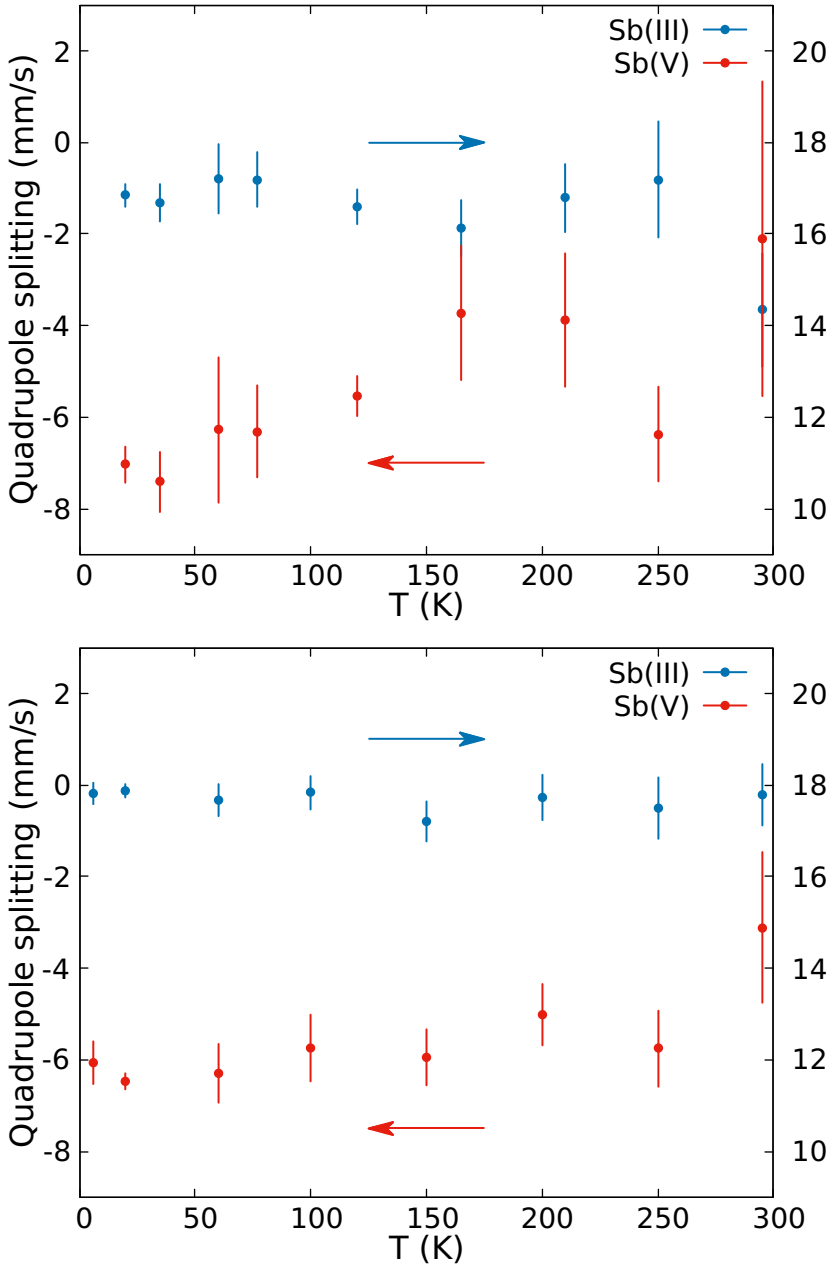

Figure S7: Temperature-dependence of quadrupole splittings of the Sb^{III} and Sb^{V} ions in (top) α- and (bottom) β-Sb_2O_4.

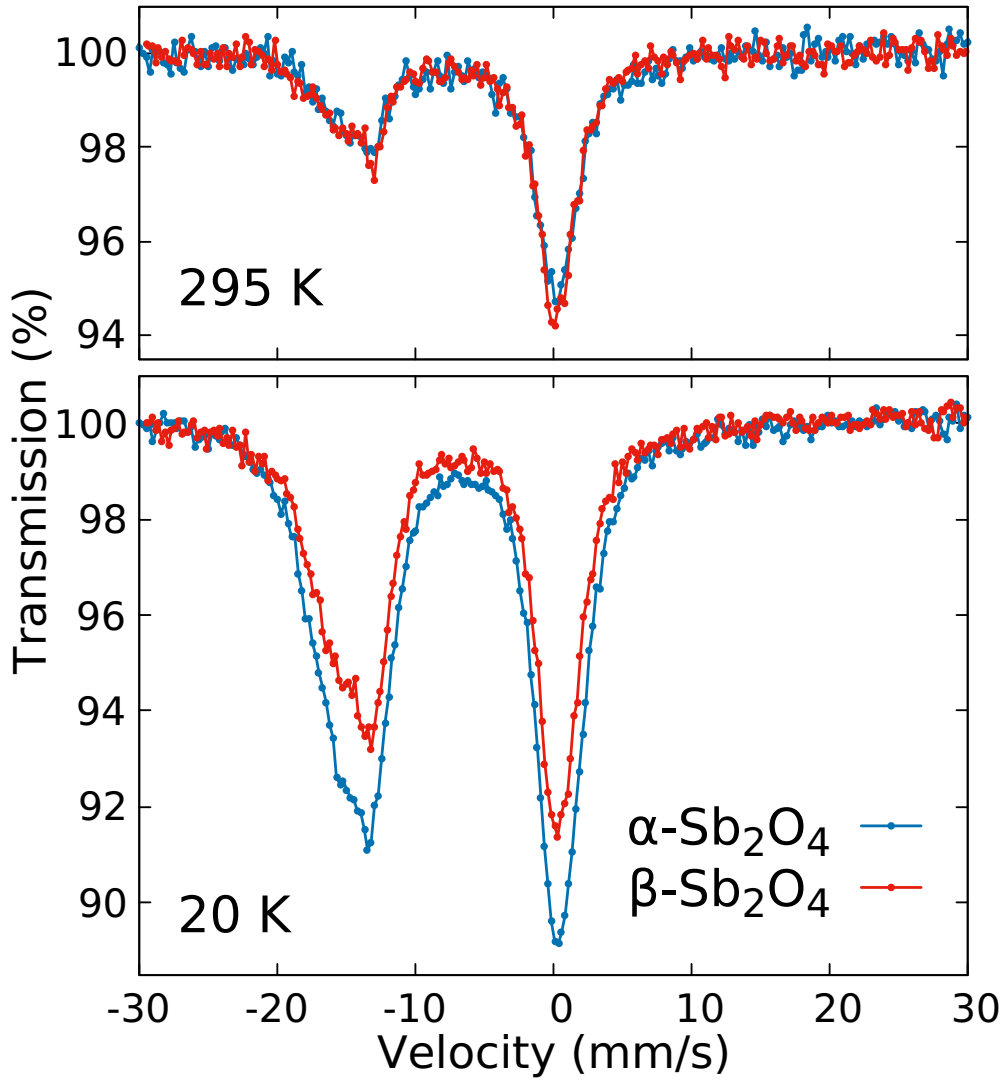

Figure S8: Illustration of softening with temperature in α- and β-Sb_2O_4 via comparison of the (top) 295 K and (bottom) 20 K Mössbauer spectra. The α phase shows more softening than the β phase, as the α phase has more intensity at 20 K (larger hardening upon cooling) and both phases are of equal intensity at 295 K.

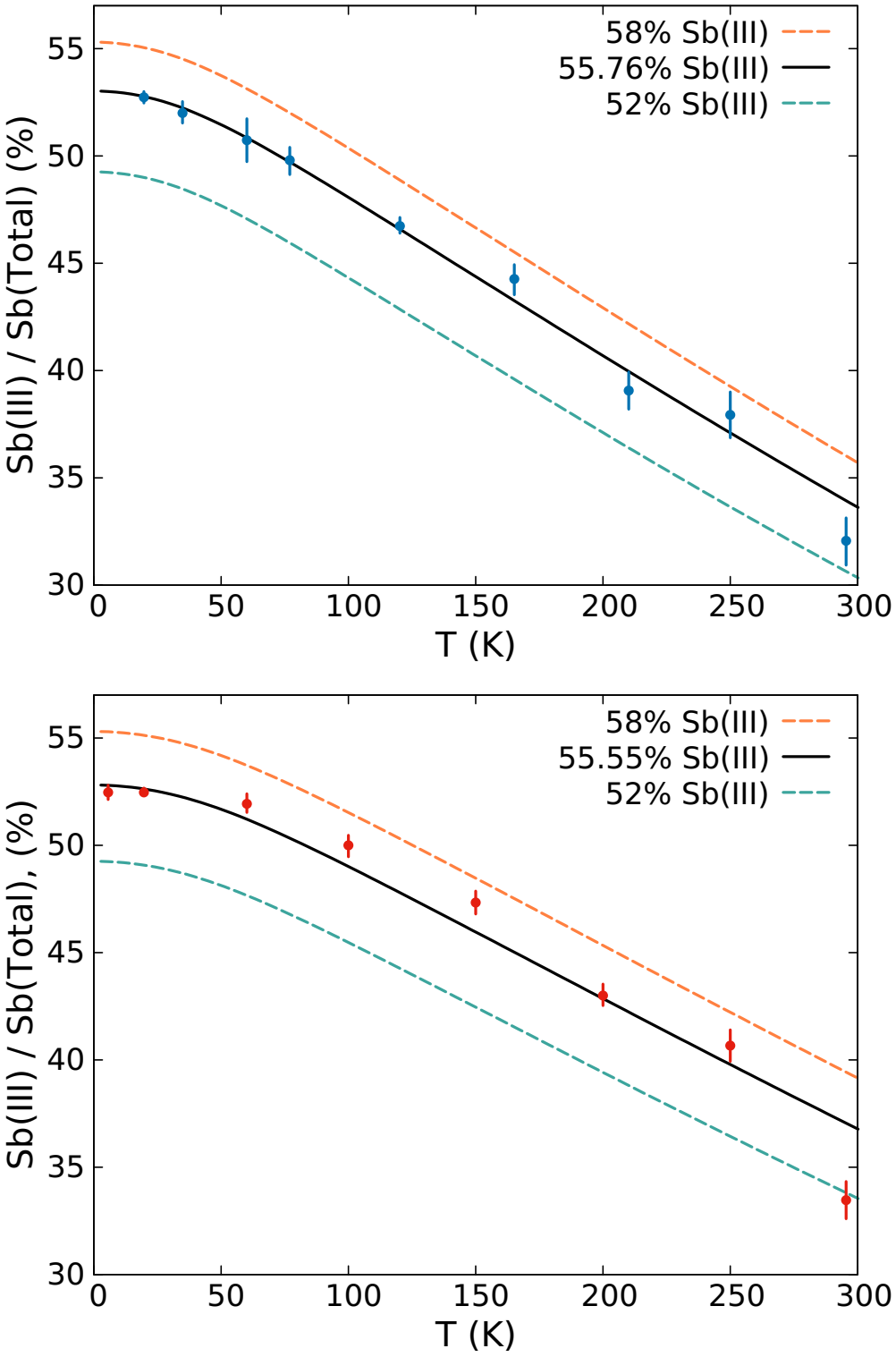

Figure S9: Apparent fraction of Sb^{III} vs total Sb in terms of peak areas. Solid black line is a fit to the observed values (blue points in [top] α-Sb_2O_4 and red points in [bottom] β-Sb_2O_4), and additional dashed lines indicate 52% and 58% fractions of Sb^{III}.

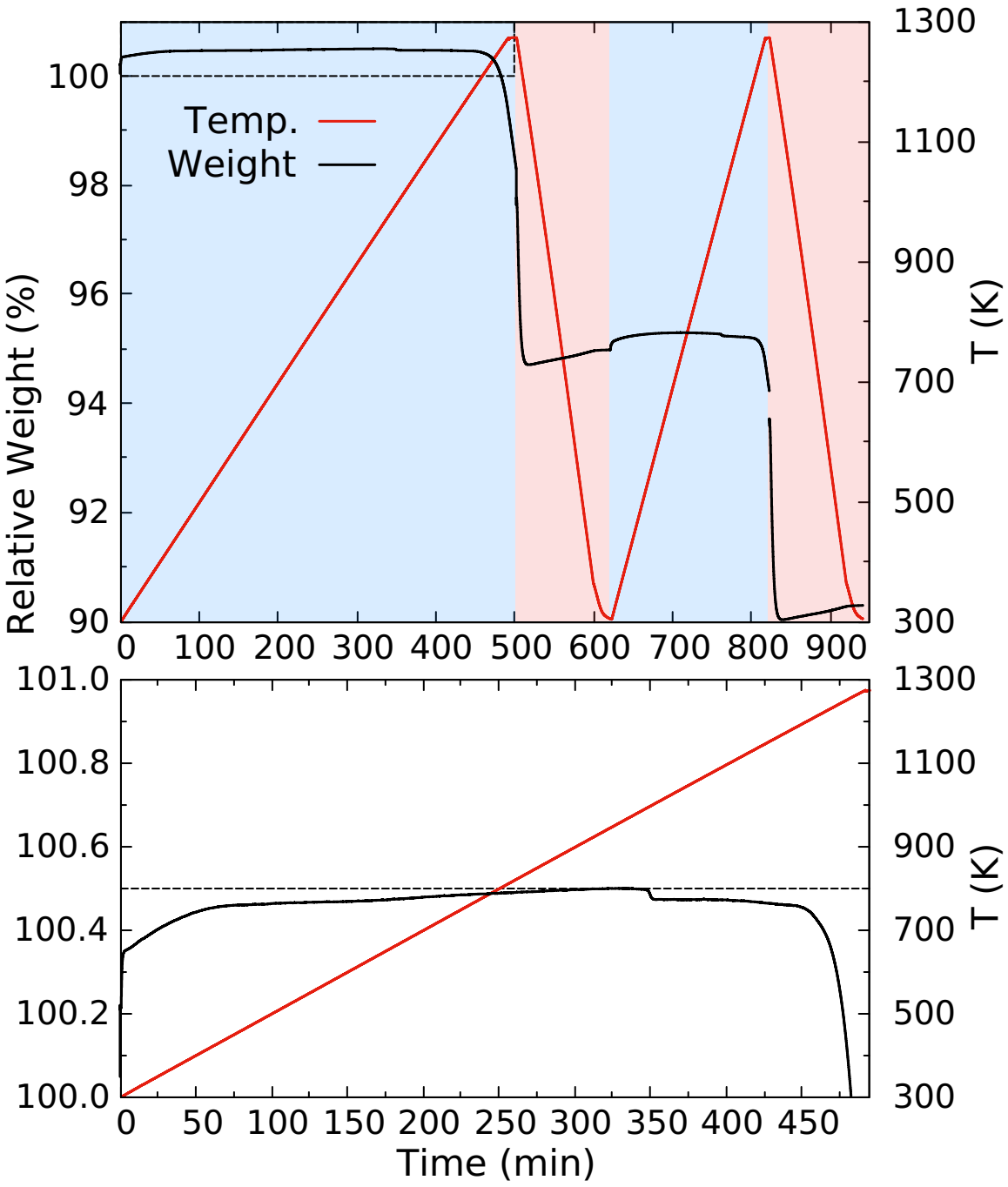

Figure S10: (top) Relative weight of α-Sb_2O_4 as a function of temperature using TGA. The red line corresponds to the temperature on the right y-axis. The blue and red regions correspond to atmospheres of pure O_2 and Ar, respectively. The region enclosed by the dashed box is enlarged in the bottom panel to show the relative weight during the initial uptake of O, which approaches 100.5% (dashed line).

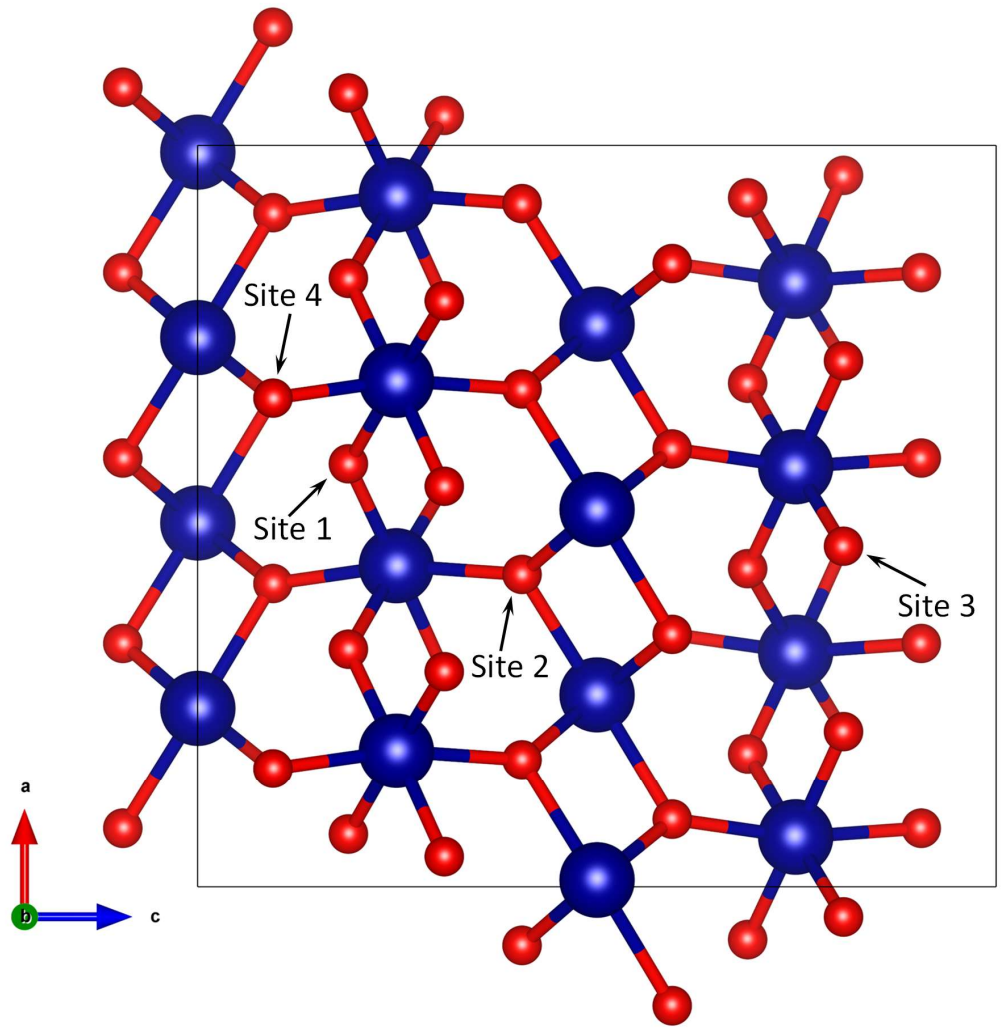

Figure S11: Supercell of α-Sb_2O_4 with chosen oxygen defect sites 1-4 indicated by arrows.

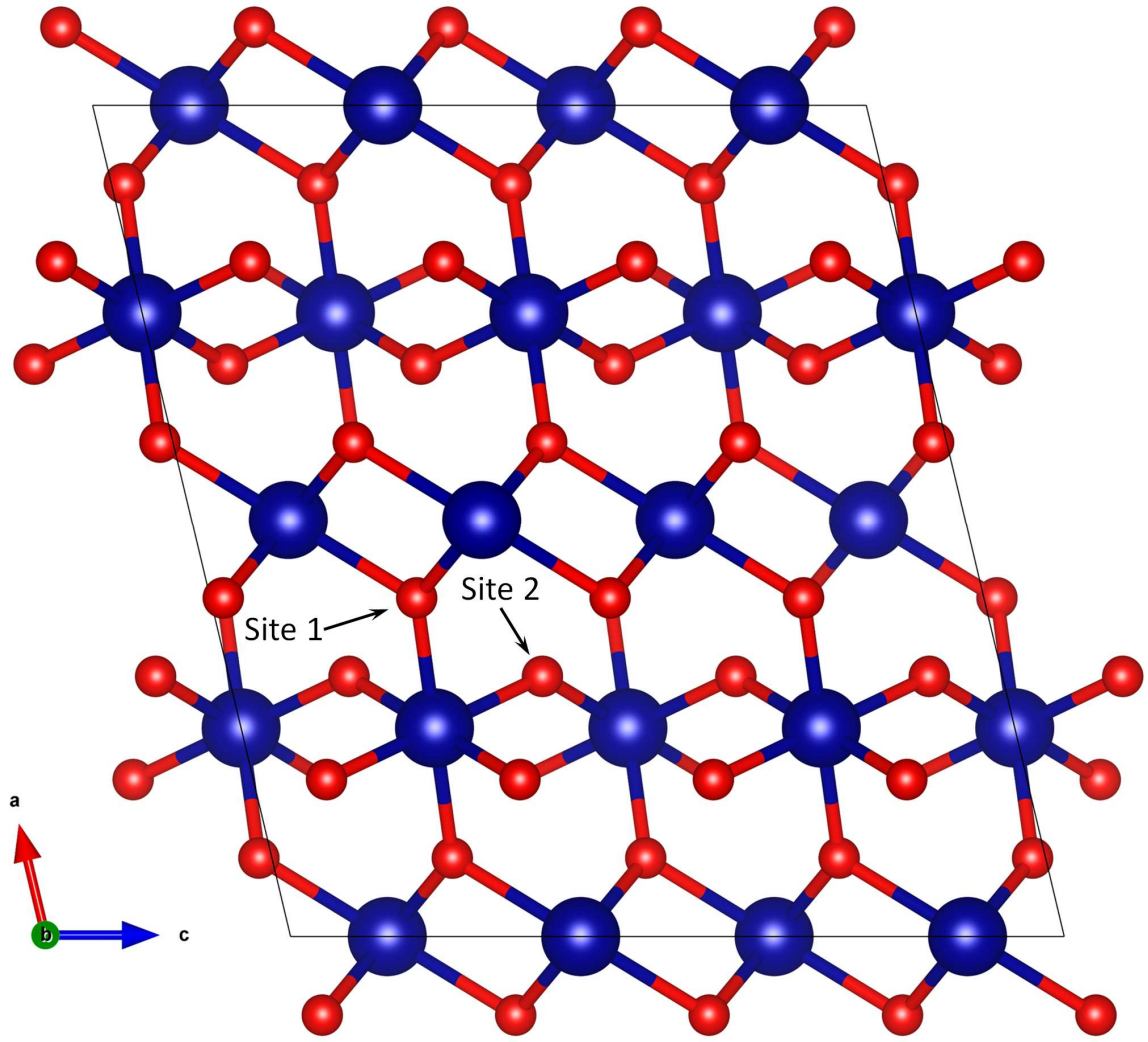

Figure S12: Supercell of β-Sb_2O_4 with chosen oxygen defect sites 1 and 2 indicated by arrows.

Table S4: Experimental Wyckoff positions and oxygen vacancy formation energies (E_F) of each nonequivalent O atom in both phases.

α-Sb_2O_4	4a Wyckoff positions			E_F (eV)
Site 1	0.1512	0.7054	0.1912	2.70
Site 2	0.3518	0.8320	0.4076	3.40
Site 3	0.0822	0.2021	0.3052	2.70
Site 4	0.3175	0.1572	0.0952	3.23
β-Sb_2O_4	8f Wyckoff positions			E_F (eV)
Site 1	0.0946	0.4132	0.9637	3.33
Site 2	0.1908	0.0516	0.6749	3.00

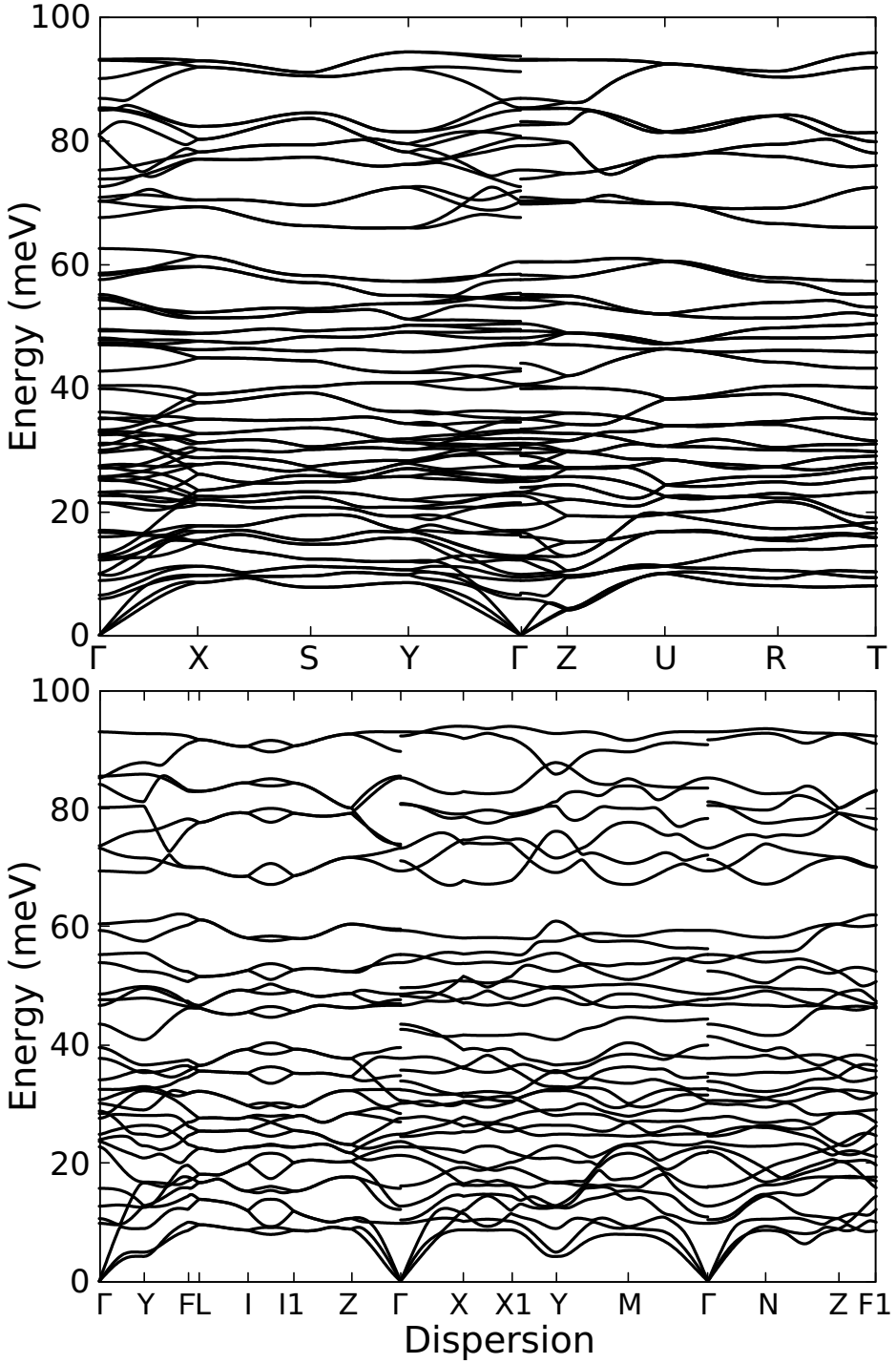

Figure S13: Calculated phonon dispersion of (top) α- and (bottom) β-Sb_2O_4.

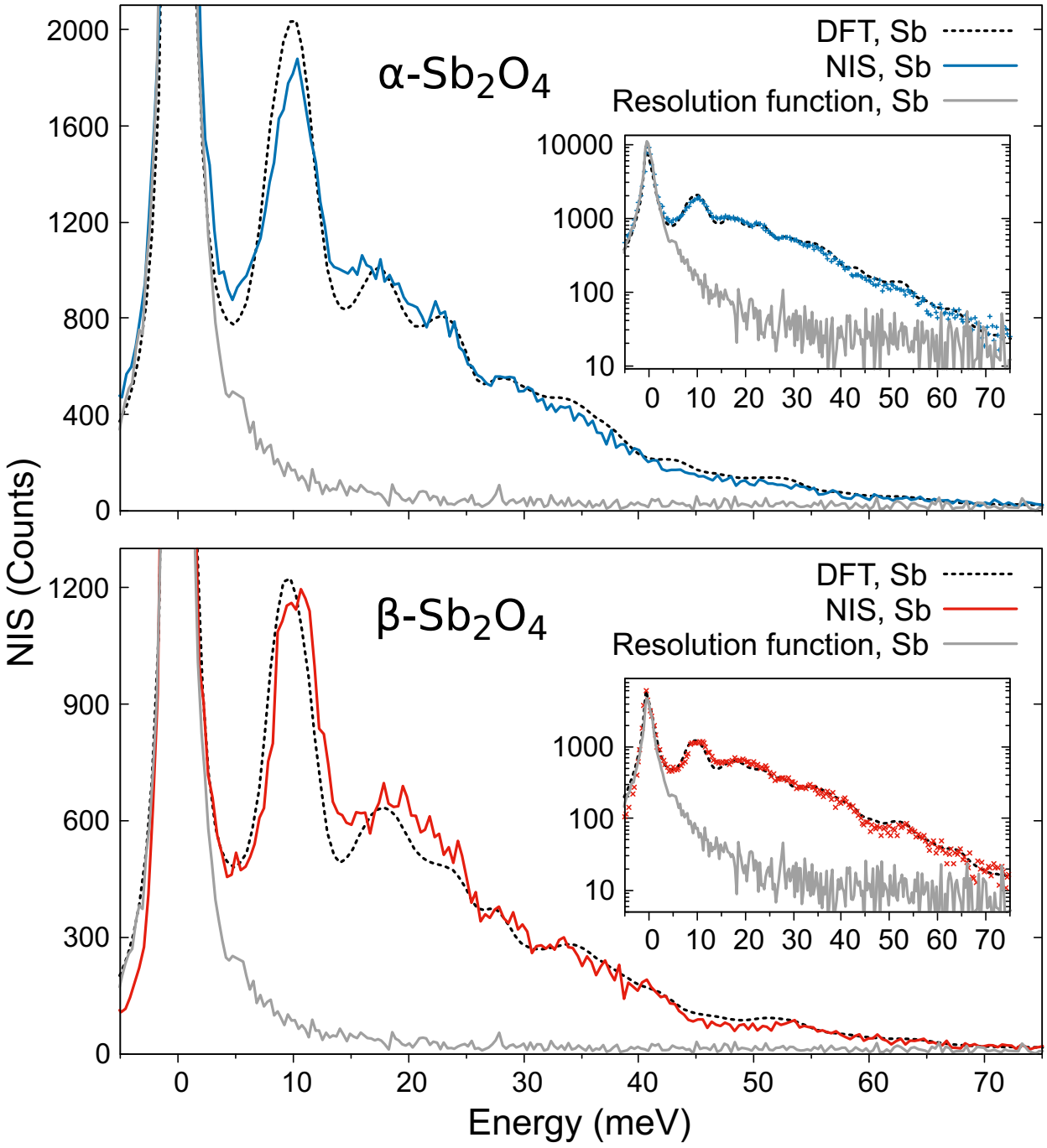

Figure S14: Element-specific ^{121}Sb NIS spectra (colored curves) and corresponding instrumental functions (gray curves) measured in (top) α-Sb_2O_4 and (bottom) β-Sb_2O_4. Insets show the same spectra in the logarithmic scale. DFT calculated ^{121}Sb NIS spectra are presented in dotted black curves. Data spread indicates error bars.

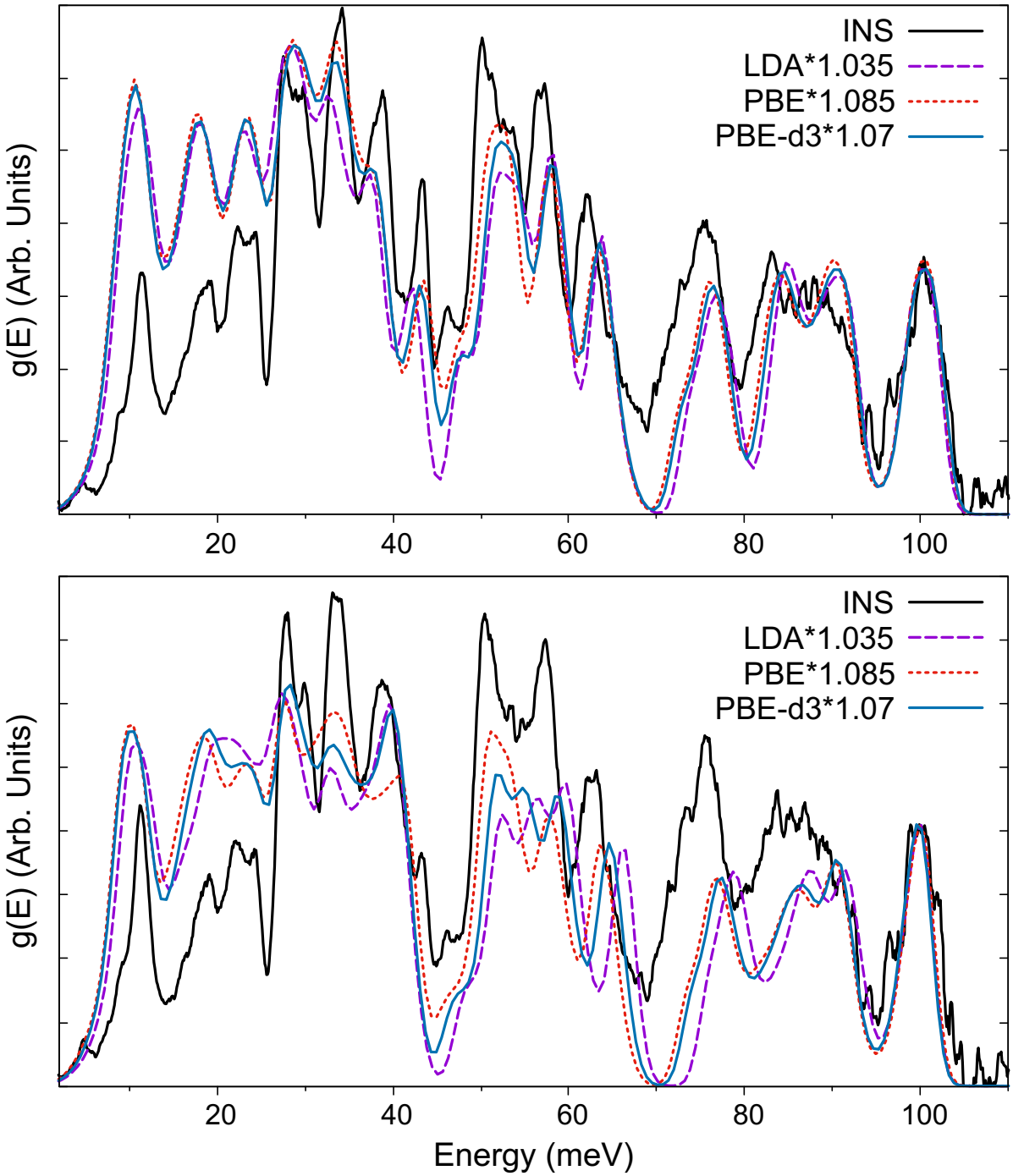

Figure S15: Comparison of the calculated DPS using different functionals of α-Sb_2O_4 (top) and β-Sb_2O_4 (bottom). The scaling factors used are listed in the legend ($g(E) \rightarrow \frac{1}{s}g(\frac{E}{s})$). All calculated spectra are scaled to match the peak at 100 meV.

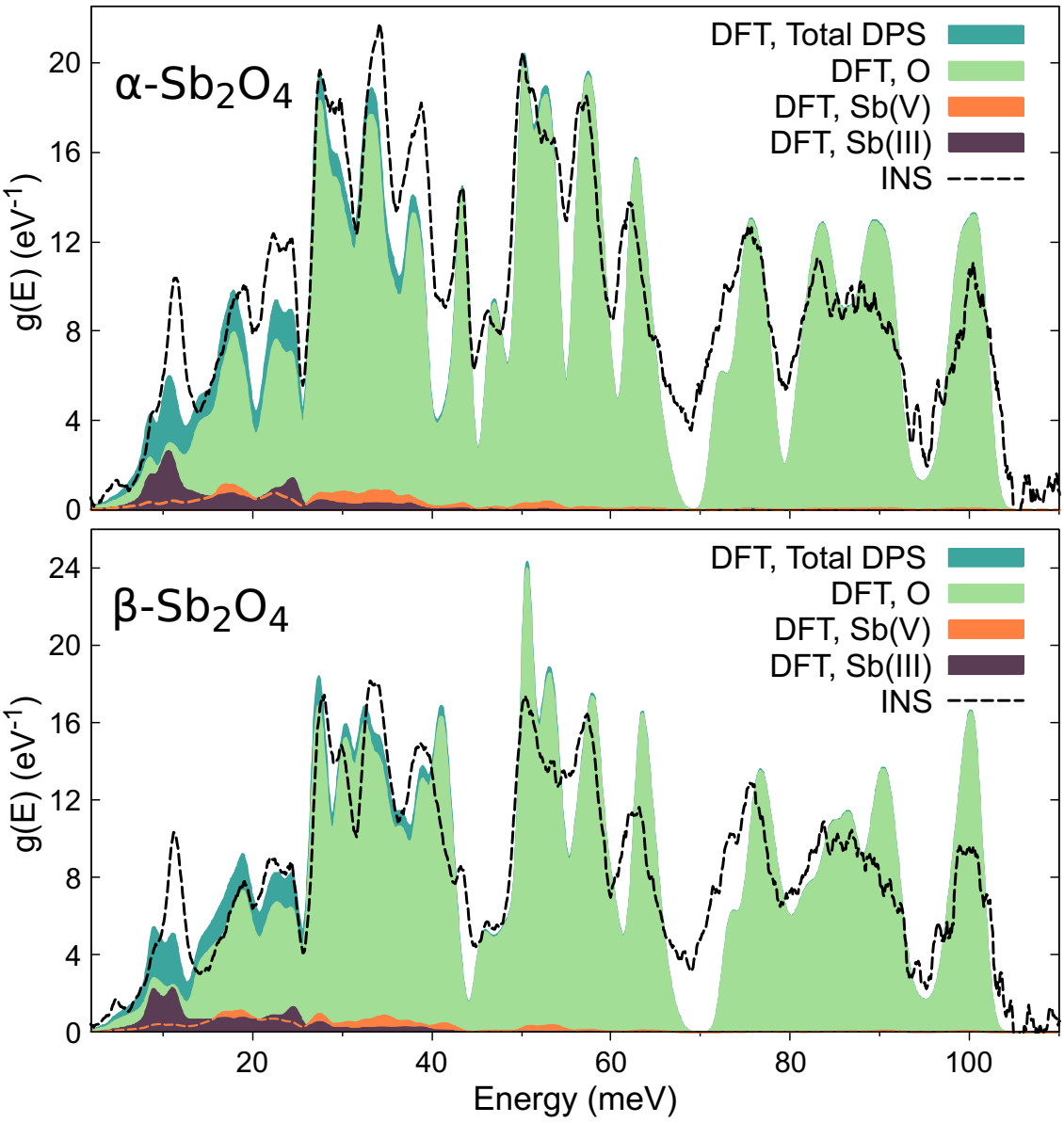

Figure S16: Neutron-weighted experimental GDPS (INS) and calculated DPS for (top) α-Sb_2O_4 and (bottom) β-Sb_2O_4. The calculated DPS have been stretched in energy by 8.5%. The filled curves in all panels show the partial O (light green), Sb^{III} (orange), and Sb^{V} (brown) DPS, as well as the total DPS (teal). The total GDPS measured by INS are shown by black dashed lines. The calculated Sb partial DPS spectrum is normalized to unity and the O-DPS to 2 in both compounds. The total DPS are the sum of weighted normalized partial DPS. The INS experimental GDPS is vertically scaled for the best match.

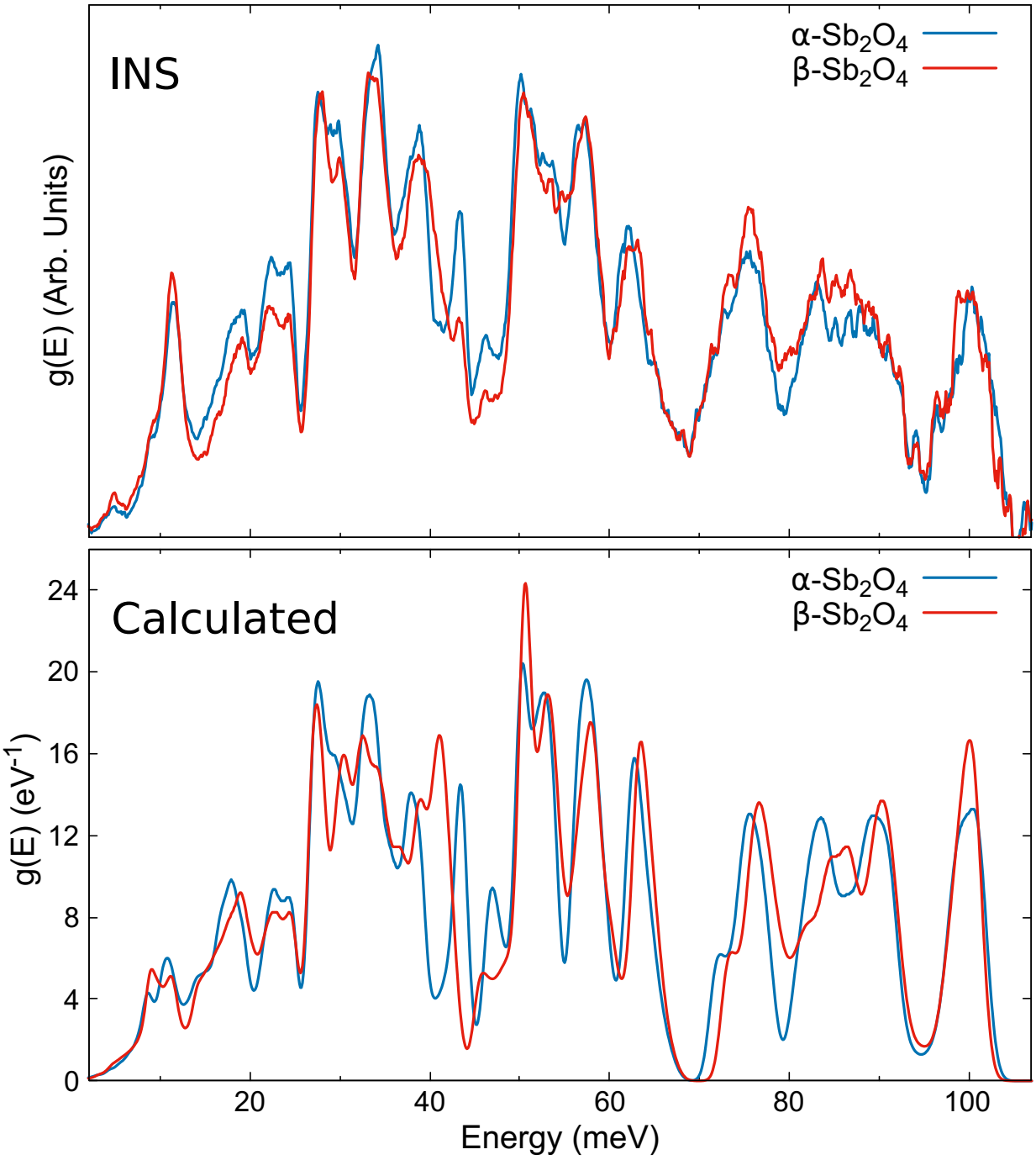

Figure S17: Comparison of α-Sb_2O_4 and β-Sb_2O_4 from (top) INS and (bottom) DFT calculations scaled in energy by 8.5%.

Table S5: Scaled energies and symmetries of calculated modes in α-Sb_2O_4.

Energy (meV)	Energy (cm^{-1})	Symmetry	Energy (meV)	Energy (cm^{-1})	Symmetry
6.395	51.578	A_2	43.776	353.080	A_2
7.036	56.754	A_1	44.027	355.105	B_1
9.599	77.421	B_2	46.339	373.752	A_1
10.178	82.092	B_1	50.943	410.886	A_1
10.676	86.108	A_1	51.243	413.306	A_2
13.184	106.337	A_2	51.297	413.742	B_2
13.454	108.515	B_1	52.154	420.654	B_2
13.602	109.708	A_2	53.380	430.542	A_2
13.929	112.346	A_1	53.658	432.785	A_1
17.246	139.100	B_2	54.658	440.850	B_1
18.022	145.358	B_1	57.418	463.111	B_1
18.417	148.544	A_2	58.850	474.661	A_1
22.864	184.412	B_1	59.258	477.952	A_2
23.241	187.453	A_1	59.797	482.299	B_2
24.489	197.519	B_2	62.395	503.254	A_2
25.027	201.858	A_1	63.180	509.585	B_2
25.090	202.366	B_1	65.545	528.660	B_1
26.952	217.384	B_1	73.286	591.096	A_1
27.168	219.126	A_1	76.118	613.938	B_1
27.432	221.256	B_2	76.158	614.261	A_2
27.693	223.361	A_2	76.832	619.697	B_2
29.322	236.500	B_2	78.716	634.893	A_1
29.699	239.541	A_2	80.054	645.684	B_2
29.717	239.686	B_2	81.633	658.420	A_2
31.925	257.495	B_1	85.887	692.731	B_1
32.050	258.503	A_1	87.566	706.273	A_1
33.374	269.182	A_1	89.536	722.162	B_1
33.688	271.714	A_2	92.134	743.117	A_1
34.500	278.264	B_1	92.332	744.714	B_2
35.600	287.136	A_2	92.542	746.408	A_2
35.739	288.257	B_2	94.194	759.732	B_1
36.004	290.394	A_1	100.86	813.497	A_2
37.902	305.703	B_1	101.05	815.030	B_2

Table S6: Scaled energies and symmetries of calculated modes in β-Sb_2O_4.

Energy (meV)	Energy (cm^{-1})	Symmetry
10.631	85.745	B_g
11.232	90.593	B_u
13.781	111.152	A_g
17.048	137.503	A_u
23.102	186.332	B_u
24.668	198.962	B_g
25.646	206.851	A_g
26.562	214.239	B_u
26.988	217.675	A_u
29.919	241.315	B_g
30.803	248.445	A_u
32.660	263.423	A_g
33.163	267.480	B_u
35.227	284.127	A_u
36.776	296.621	B_u
40.922	330.061	B_g
42.897	345.990	A_u
46.249	373.026	B_u
50.642	408.459	A_g
51.697	416.968	A_u
52.720	425.219	B_g
53.914	434.849	B_u
58.495	471.798	A_g
59.990	483.856	B_g
64.401	519.433	A_u
75.319	607.497	A_g
77.195	622.625	B_u
79.515	641.337	B_g
79.968	644.991	A_u
87.723	707.540	B_u
92.412	745.359	A_g
92.740	748.005	A_u
100.86	813.497	B_g

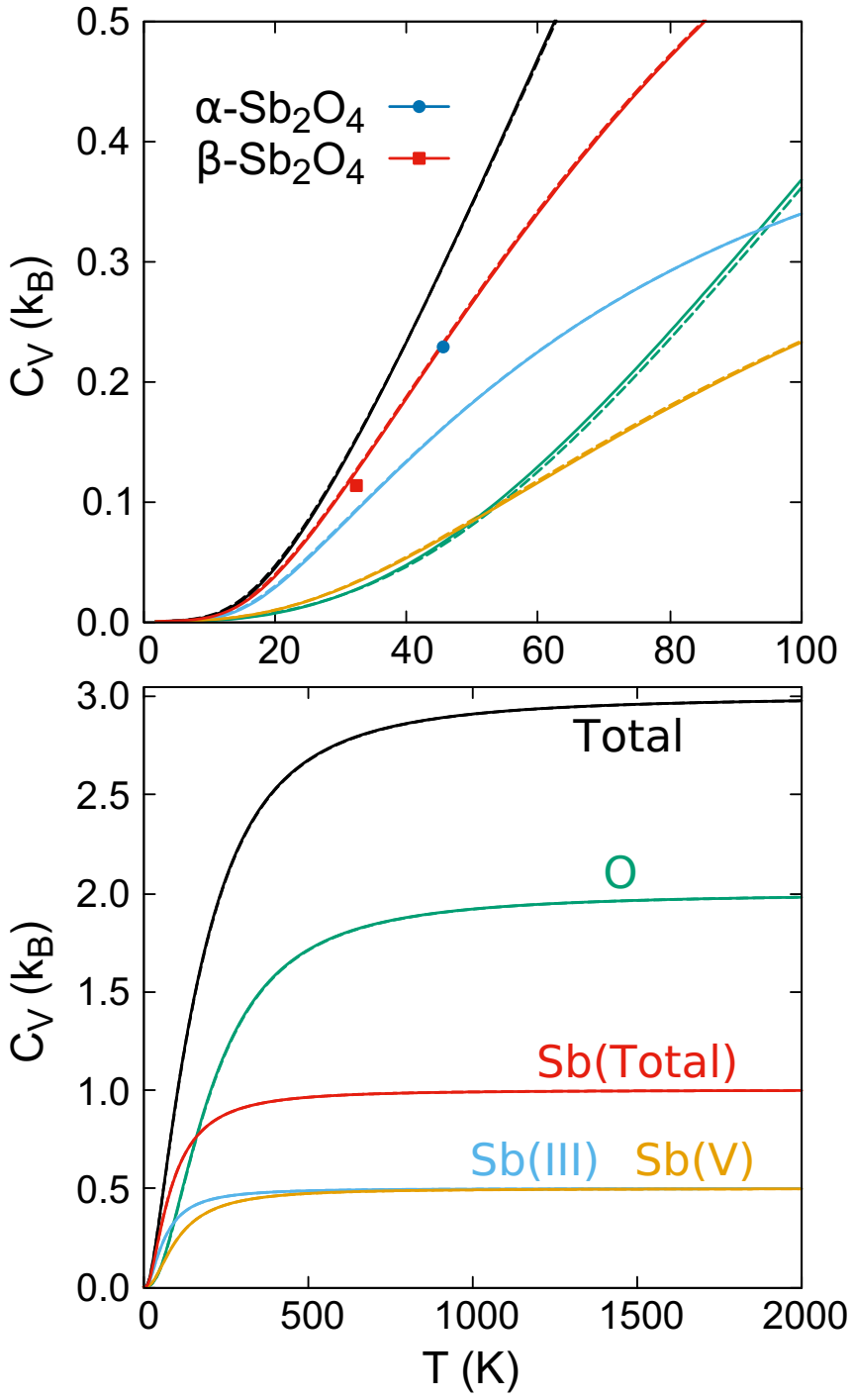

Figure S18: Temperature-dependence of the heat capacity of constituent atoms of α-Sb_2O_4 within the harmonic approximation. β-Sb_2O_4 values are presented as dashed lines. Data points in top plot correspond to C_V extracted from NIS data.

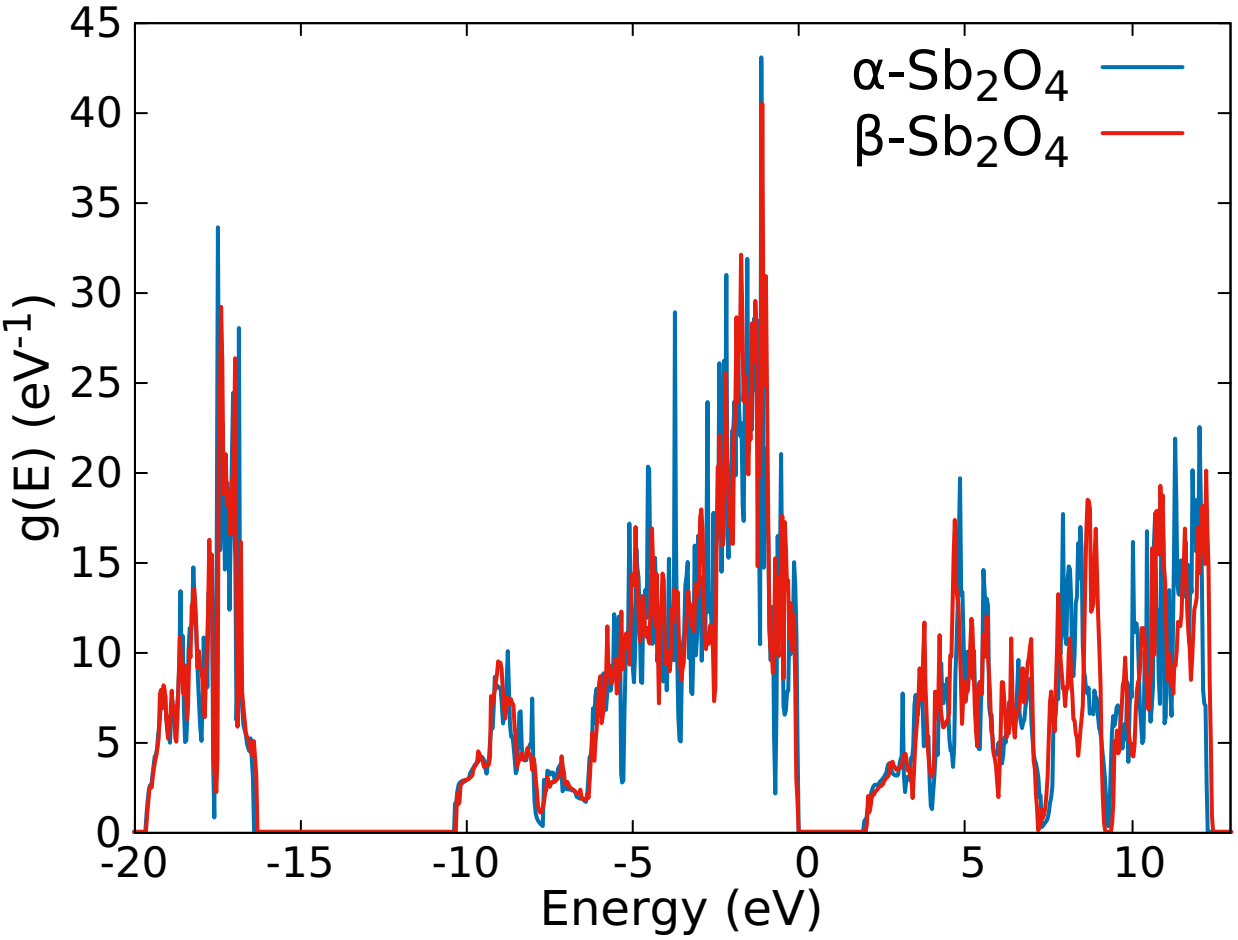

Figure S19: Comparison of the calculated electronic DOS of α-Sb_2O_4 (blue) and β-Sb_2O_4 (red).